Proceedings of the 30th International Cosmic Ray Conference
Rogelio Caballero, Juan Carlos D'Olivo, Gustavo Medina-Tanco,
Lukas Nellen, Federico A. Sánchez, José F. Valdés-Galicia (eds.)
Universidad Nacional Autónoma de México,
Mexico City, Mexico, 2008

Vol. 4 (HE part 1), pages 377–380

30TH INTERNATIONAL COSMIC RAY CONFERENCE

Composition-sensitive parameters measured with the surface detector of the Pierre Auger Observatory

M.D. HEALY[1] FOR THE PIERRE AUGER COLLABORATION[2]
[1]*University of California, Los Angeles, Los Angeles, CA 90095, USA*
[2]*Observatorio Pierre Auger, Av. San Martín Norte 304, (5613) Malargüe, Argentina*
healymd@physics.ucla.edu

Abstract: A key step towards the understanding of the origin of ultra-high energy cosmic rays is their mass composition. Primary photons and neutrinos produce markedly different showers from nuclei, while showers of different nuclear species are not easy to distinguish. To maximise the discrimination with the Pierre Auger Observatory ideally all mass-sensitive observables should be combined, but the 10% duty cycle of the fluorescence detector limits the use of direct measurements of shower maximum at the highest energies. Therefore, we investigate mass-sensitive observables accessible with the surface detectors alone. These are the signal risetime in the Cherenkov stations, the curvature of the shower front, the muon-to-electromagnetic ratio, and the azimuthal signal asymmetry. Risetime and curvature depend mainly on the depth of the shower development in the atmosphere, and thus on primary energy and mass. The muon content of a shower depends on the primary energy and the number of nucleons, while asymmetry about the shower core is due to geometric effects and attenuation, which are dependent on the primary mass. The mass sensitivity of these variables is demonstrated and their application for composition studies is discussed.

Introduction

The Pierre Auger Observatory [1, 2] records air showers induced by cosmic rays with energies $> 10^{18}$ eV with unprecedented precision and statistics. Key to this are the shape of the energy spectrum, the arrival direction distribution and the composition of the primaries. Specifically, a transition of galactic to extragalactic cosmic rays could be indicated by a marked change of composition (see e.g. [3, 4, 5]). While the determination of the direction and energy of cosmic rays are relatively easy , the determination of the identity of primary particles from the details of the atmospheric extensive air showers (EAS) is difficult. Differences between neutrino and photon induced showers and those initiated by nuclei are relatively easy to detect [6, 7, 8]. The differences between nuclear species (e.g. proton and iron) are more difficult to measure: on average heavier nuclei (of the same total energy) develop higher in the atmosphere (lower $X_{\max}$), due to their larger cross-sections and the lower energy per nucleon, produce more secondary particles, and have a higher muon-to-electron ratio at observation level. These differences are small and easily concealed by the variations due to the primary energy or by uncertainties in hadronic interaction models, and are covered by shower fluctuations and the limited precision of the measurement with a realistic detector. The Pierre Auger Observatory is a hybrid detector, combining a large array of water-Cherenkov detectors (surface detector, SD, with 100% duty cycle) and 24 fluorescence telescopes (FD, with 10% duty cycle). Hybrid events have a good energy estimate and provide a direct measurement of $X_{\max}$. But 90% of the events have information only from the surface array and, therefore, observables from the array are needed for composition analysis at the highest energies. In the following we discuss four observables which all rely on the time structure of the shower front as measured with a 25 ns flash ADC system (FADC) of the water-Cherenkov detectors. They are all sensitive to the primary mass, via their dependence on the height of shower development and the muon content in the shower: **(i)**

The signal risetime in water tanks at some distance from the shower core depends mainly on the height of the shower development: the higher the shower development in the atmosphere, the smaller the time spread between the particles and the smaller the risetime. (**ii**) The curvature of the shower front reflects the height of the shower development: the further the main shower development from the detector, the flatter the shower front. (**iii**) The muon content of a shower can be assessed by looking for tell tale signs of sudden, large energy deposits in the time traces, as they are expected from muons: the frequency of large jumps in the signal from one FADC bin to the next relates to the abundance of muons. (**iv**) The azimuthal asymmetry in the signal risetimes within the shower plane is an effect of a varying muon-to-electromagnetic component, and as such it depends on the shower development and the muon content.

While all of these variables could in principle be used for composition studies with a perfect detector, there are limitations due to the finite accuracy with which they can be measured. Therefore, it needs to be shown that measurement uncertainties are small enough that the mass differences can be detected reliably. Once the mass sensitivity of the individual variables is established, a multivariate analysis method will be needed to combine all mass-sensitive observables to maximise the mass separation power. A combination of risetime and curvature has already been used successfully to pose an upper limit on primary photons [7].

The risetime of the signal, $\mathbf{t}_{1/2}$

The signals in the 10 m^2 water-Cherenkov detectors are characterised by $t_{1/2}$, the time to rise from 10 to 50% of the integrated signal. The signals, up to 3 μs long, are recorded with a 25 ns FADC system. The risetime in an individual station depends on core distance, zenith angle and energy and has been parameterised from experimental data to correct events from different zenith angles. The measurement uncertainty $\sigma_{t_{1/2}}$ as function of signal S in the tank, the core distance r and zenith angle θ has been determined from a small number of twin tanks and from pairs of detectors at similar core distances (within 100 m). A parameterisation of $\sigma_{t_{1/2}}$ is used to define the error bars shown in fig. 1 (top). Measurements of $t_{1/2}$ for signals < 20 VEM are severely influenced by Poisson fluctuations due to low numbers of particles and are not used. A correction of the risetime for the azimuthal asymmetry in the shower, particularly important between 35 and 50°, is applied. For each station the deviation Δ of the measured risetime, in units of the accuracy of measurement, from the average values found for r and θ at a fixed reference energy $E \approx 10^{19}$ eV is formed, thus: $\Delta = \frac{t_{1/2}(r,\theta) - \langle t_{1/2}(r,\theta,E_{\rm ref})\rangle}{\sigma_{t_{1/2}}(S,r,\theta)}$. All stations in one event are then combined in an average event deviation $\langle\Delta\rangle$ as seen in fig. 1 (top), which should

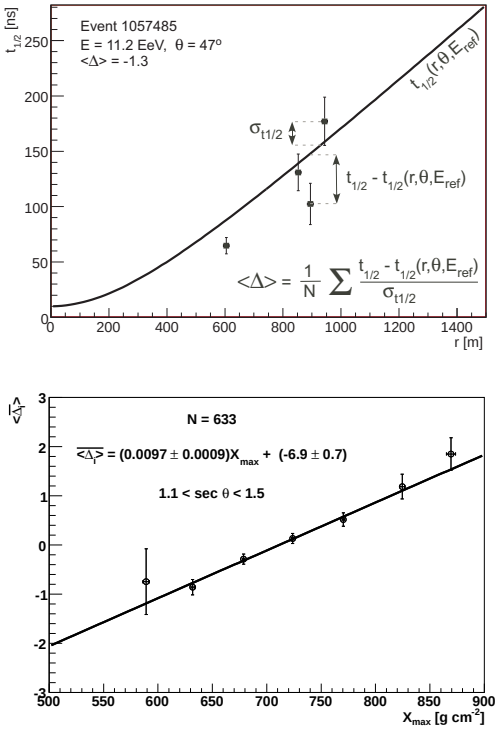

Figure 1: **Top:** $\langle\Delta\rangle$ derived from a single event. The black line is the predicted risetime while the data points represent measurements with the error bars from twin station studies. Combining each stations' Δ from the expectation an average for the event can be defined. **Bottom:** $\overline{\langle\Delta\rangle}$ as a function of $X_{\rm max}$, for nearly-vertical hybrid events.

be larger for showers developing deeper than the reference and smaller for those developing higher. Using hybrid events [9] it can be tested whether the so-constructed variable $\langle\Delta\rangle$ indeed correlates with $X_{\rm max}$. The data have been binned in $X_{\rm max}$, and for all events in one $X_{\rm max}$ bin the average of $\langle\Delta\rangle$ (i.e. $\overline{\langle\Delta\rangle}$) has been formed. This is shown in fig. 1 (bottom). A linear dependence is observed which allows estimation of $X_{\rm max}$ from events observed with the SD alone.

Shower Front Curvature

The trigger times of the array detectors away from the core lag behind what one would expect from a plane of particles traveling at the speed of light, indicating the shower front is curved. With the assumption of a hemispherical shower front a *radius of curvature*, $\mathrm{R_c}$, can be derived. The radius of curvature is an SD observable that Monte Carlo simulations show is mass sensitive (see Fig. 2). Larger distances of $X_{\rm max}$ from the array yield larger radii of curvature, while deeply penetrating showers produce shower fronts with smaller radii of curvature. Also muons tend to travel in straight lines and electrons are more scattered, so muons arrive at the detectors first, and with a narrower time spread, as compared to the electro-magnetic component. Therefore, a shower with a larger number of muons will produce station triggers that are compact in time, resulting in a flatter shower front than for a similar shower that is muon-poor. The radius of curvature is strongly dependent on zenith angle because the distance from the array to shower maximum increases with zenith angle ($\propto (X_0 \sec\theta - X_{\rm max})$). Fig. 2 demonstrates the typical resolution between the radius of curvature and changes in $X - X_{\rm max}$.

Muon Content

As a typical muon deposits much more energy ($\approx$ 240 MeV) in a water tank than an electron or photon ($\approx$ 10 MeV), spikes are produced over the smoother electromagnetic background in the FADC time traces. Thus, muons manifest themselves as sudden variations in the signal ΔV from one FADC bin to the next. The expected distributions of ΔV for purely electromagnetic and muonic traces look very different. A mix of electromagnetic and muonic signals is needed to fit the measured distribution (see Fig. 3). The number of muons in the shower is then estimated via the number of ΔVs above 0.5 VEM with $N_\mu = \alpha N(\Delta V > 0.5\mathrm{VEM})$; with $\alpha \approx 1.4$ being only weakly dependent on core distance and zenith angle. The N_μ resolution is about 25%, systematic errors are below 10%.

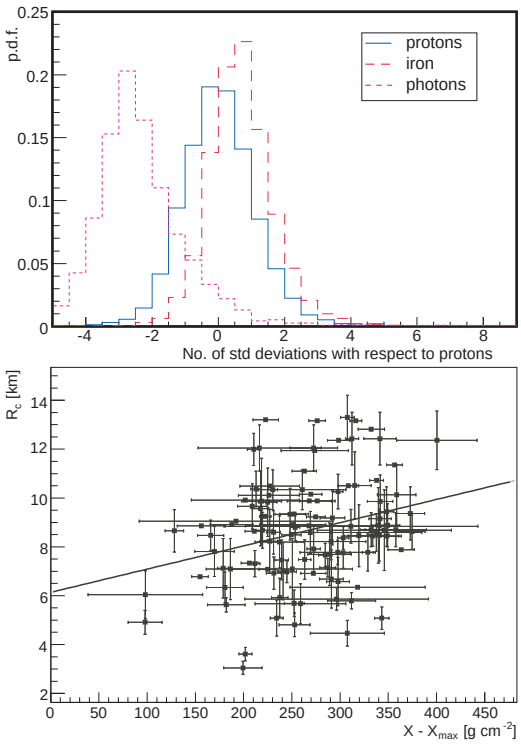

Figure 2: **Top:** Comparative radii of curvature from simulations of three primaries (solid-blue: proton, solid-red: iron, dashed-magenta: photon). **Bottom:** $\mathrm{R_c}$ is shown as a function of $X - X_{\rm max}$ for nearly vertical hybrid showers ($1.1 < \sec(\theta) < 1.2$). The line is a linear fit to the data points correlating $\mathrm{R_c}$ with the distance from the detector to the shower maximum.

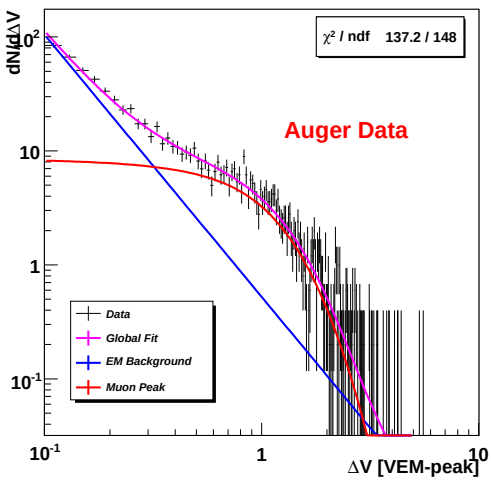

Figure 3: Distribution of jumps for Auger events with energy between 8-12 EeV and 40-50°, averaged over 251 stations - 100 showers - within the same core distance interval.

Azimuthal Asymmetry

The observed azimuthal asymmetry in the risetimes offers another handle on primary composition determination. Its magnitude is a measure of the degree of shower development and hence it is sensitive to primary composition [10]. The dependence of the risetimes with azimuthal angle ζ is fitted using $t_{1/2}(r,\zeta) = a + b\cos\zeta$, for all stations with 500 m $< r <$ 2000 m and with signals greater than 10 VEM. The asymmetry factor $\frac{b}{a}$ is sensitive to the distance between the detector and the shower maximum (shown in fig. 4 as $\sec\theta \propto X - X_{\max}$). Maximal asymmetry occurs at a unique value of $X - X_{\max}$ found most frequently at a corresponding zenith angle. Monte Carlo simulations show that this zenith angle (θ_{asymax}) is different for proton and iron showers (Fig. 4) reflecting the systematic difference in the average $X_{\max}$.

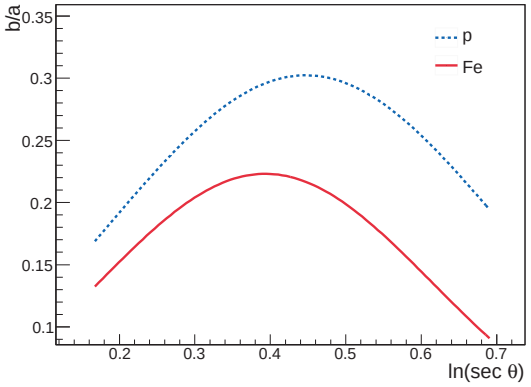

Figure 4: Development of the asymmetry factor in the risetime with zenith angle. The primary energy is $\sim 10^{18.5} eV$.

References

[1] J. Abraham *et al.* [P. Auger Collaboration], Nucl. Instr. Meth. A 523 (2004) 50–95.

[2] J. Abraham *et al.* [P. Auger Collaboration], in: Proc. 30th ICRC (Mérida), 2007.

[3] A. M. Hillas, J. Phys. G 31 (2005) 95.

[4] V. Berezinsky *et al.*, Phys. Rev. D. 74 (2006) 61.

[5] D. Allard *et al.*, Astrop. Phys. 27 (2007) 61.

[6] J. Abraham *et al.* [P. Auger Collaboration], Astrop. Phys. 27 (2007) 155.

[7] J. Abraham *et al.* [P. Auger Collaboration], Submitted to Astrop. Phys.

[8] O. Blanch *et al.* [P. Auger Collaboration], in: Proc. 30th ICRC (Mérida), 2007.

[9] M. Unger *et al.* [P. Auger Collaboration], in: Proc. 30th ICRC (Mérida), 2007.

[10] M. T. Dova *et al.*, in: Proc. 29th ICRC (Pune), 2005, pp. 101–104.